Axial Mixing in Modern Packings, Gas and Liquid Phases: I. Single-Phase Flow

Ricardo Macías-Salinas and James R. Fair
Separations Research Program, Dept. of Chemical Engineering, The University of Texas at Austin, Austin, TX 78712

An experimental study was conducted in a 0.43-m-ID packed column to determine the axial mixing properties of air and water under single-phase flow conditions. The packings used were 25.4-mm ceramic Raschig rings, one modern random packing, 25.4-mm metal Pall rings; two structured packings, Sulzer BX and Flexipac 2. The column was operated at ambient conditions with flow rates varying from 0.4 to 4 kg/m^2 · s for the gas and from 3.25 to 8.5 kg/m^2 · s for the liquid. Axial mixing was experimentally determined via dynamic response studies based on the pulse injection technique. The diffusion-type model served to reproduce the experimental response curves satisfactorily and proved to be a suitable means of describing axial mixing in both phases. The results confirm previous observations for first-generation packings. Axial mixing is much greater in the liquid than in the gas; axial mixing in the gas increases with gas rate, whereas axial mixing in the liquid decreases with liquid rate. It was also found that the two structured packings produce the lowest levels of axial mixing in the gas. Surprisingly, the greatest mixing effects in the liquid were obtained for Flexipac 2 structured packing. Correlations were developed to represent the experimental mixing and liquid holdup data, yielding an average ± 16% difference between experimental and correlated data. Mixing measurements in gas or liquid under two-phase flow conditions will be discussed in Part II.

Introduction

An understanding of nonideal flow behavior in packed beds is important in the study of transport processes conducted in the beds. An important nonideal flow phenomenon in columns filled with packing elements is axial dispersion, or longitudinal mixing. This behavior represents a deviation from plug flow and influences adversely the axial concentration profile in the flowing streams; the result is a decrease in concentration driving forces and poorer separation efficiency. In general, this departure from plug flow mainly results from viscous effects, molecular diffusion as in laminar flow, and eddy diffusion for turbulent flow. Although packings can reduce axial dispersion, it is well established that under certain operating conditions (high flow rates, and high pressure), severe axial dispersion in a flowing stream may occur in packed beds.

Correspondence concerning this article should be addressed to R. Macías-Salinas at his preent address: Instituto Politécnico Nacional, ESIQUE-UPALM, Zacatenco, Mexico, D.F. 07738.

Axial dispersion for single-phase flow through first-generation random packings has been extensively studied. For the case of modern random or structured packings, however, the work by Mak et al. (1991) is probably the only experimental study that has been reported. Specifically, the aim of the present investigation is two-fold: (1) to develop a suitable experimental approach for measuring gas- and liquid-phase axial dispersion in a large-scale column containing modern random or structured packing; and (2) to provide correlated experimental data of axial dispersion coefficients in each phase together with liquid-phase holdup data, through the application of dynamic response techniques.

Experimental Studies

During the last four decades, much effort has gone into the study and interpretation of axial dispersion properties of single-phase flow through packed beds. A large number of studies were conducted in cylindrical columns filled with

first-generation random packings such as Raschig rings and Berl saddles. In all cases the dynamic response approach was used experimentally. Response data were reproduced by means of a diffusion-type model. A detailed review of these works reveals in some cases major discrepancies in the magnitude of dispersion data reported. The use of different experimental techniques of injecting and detecting the tracer, as well as inaccuracies inherent in the method of data analysis, may explain such discrepancies.

Danckwerts (1953) along with Kramers and Alberda (1953) appear to be the first investigators to study the effects of axial dispersion in packed columns. Most of Danckwerts' work is devoted to a theoretical discussion of residence time distribution in continuous flow systems. He reported only a single dispersion experiment in a packed bed. In this experiment, he determined an axial dispersion coefficient for the flow of water through Raschig rings at a single Reynolds number. His approach involved the response of the system to a step change in concentration in the inlet. Using a frequency response technique, Kramers and Alberda (1953) presented two experimental results in a system similar to that of Danckwerts. They observed that mixing of the liquid was increased with increasing liquid velocity.

McHenry and Wilhelm (1957) reported axial mixing data of two binary gas mixtures in a bed of spherical beads. They used a sinusoidal input signal and determined values of axial dispersion coefficient from the amplitude change. For both mixtures, no significant effect of gas composition on Péclet number Pe ($\nu d_p/D_e$) was found. Employing the frequency response method and the pulse function approach, Ebach and White (1958) investigated the mixing characteristics of water and glycol-water flow through randomly packed beds. They found no significant effect of liquid viscosity, bed length and particle shape on the axial dispersion coefficient D_e (m^2/s).

Additional mixing studies of water flowing through packed beds were conducted by Carberry and Bretton (1958) over a wider range of flow rates. They also reported dispersion characteristics of a gas system in the Reynolds number Re ($\nu_s L^* \rho/\eta$) range below that studied by McHenry and Wilhelm. Their studies clearly showed significant liquid dispersion for $Re < 200 \rightarrow 300$. Beyond the transition region, the resulting liquid Péclet numbers showed a limiting value of 2 (turbulent region). For the gas phase, Carberry and Bretton concluded that the dispersion mechanism was a function of both molecular diffusion (at low Re) and turbulence. Strang and Geankoplis (1958) used a frequency response method to obtain axial dispersion data for liquid flowing through beds of three different lengths, using random packings as well as porous particles. At constant velocity, they observed no effect of frequency on dispersion, but a large effect of fluid velocity on D_e. No correction procedure was provided to account for end effects.

In an attempt to eliminate end effects in the determination of liquid dispersion data, Liles and Geankoplis (1960) proposed a method of correcting for this anomalous behavior. Their results showed a marked difference from those of Strang and Geankoplis. When end effects were intentionally imposed, large effects of length on D_e were found (D_e decreased as the length of the bed was increased). Cairns and Prausnitz (1960) investigated axial mixing properties for water flowing through a bed of glass spheres. Using the Einstein statistical model, they determined values of the axial dispersion coefficient over the range of $0.163 < Re < 162$. Their dispersion coefficients were somewhat lower than those of other investigators.

In another attempt to extend the range of experimental variables for liquid dispersion, Kunugita et al. (1962) conducted transient response studies for water flowing through random packings. They examined the effect on liquid holdup and axial dispersion of packing size and type, as well as of the ratio of packing diameter to column diameter. They found no significant effect of these variables on the mixing parameters. In an effort to correlate and interpret liquid axial dispersion at low Reynolds numbers, Miller and King (1966) reported Péclet numbers for the turbulent-laminar transition region. They found no major trend of Péclet number with either packing size or column diameter/packing diameter.

Evans and Kenney (1966) reported axial dispersion data for five binary gas mixtures flowing through packed beds. They found that, at the lowest flow rates ($Re_p < 1$) molecular diffusion was the controlling factor affecting dispersion. They also observed that at very low flow rates (up to $Re_p \approx 0.1$), viscous forces predominated and the dispersion coefficients were proportional to the interstitial velocity. Edwards and Richardson (1968) presented experimental measurements of axial dispersion of air through nonporous particles. Unlike Evans and Kenney, these investigators covered a wide range of Reynolds numbers (0.008 to 50). Their results indicated that, at low Reynolds numbers (< 1), the dispersion is only affected by molecular diffusion, but, at higher Reynolds numbers (> 10), eddy diffusion predominates. Their values of Péclet number (≈ 2) at high Reynolds numbers agreed well with those obtained by McHenry and Wilhelm (1957) and DeMaria and White (1960).

In order to extend the range of available gas-phase dispersion data, Urban and Gomezplata (1969) investigated the dispersion behavior of three binary gas mixtures flowing through a randomly packed column. They concluded that in the absence of wall effects, values of the Péclet number can surpass the limiting value of 2, especially when large packing diameters are used. They also suggested that the irregularities of particle shape tend to yield an extensive variation in local residence time owing to the formation of channels (as previously pointed out by Edwards and Richardson, 1968). In a more recent investigation, Tan and Liou (1989) studied axial dispersion of carbon dioxide flowing under supercritical conditions. They found the axial dispersion coefficient to increase with interstitial velocity and packing diameter, but to decrease with increasing pressure and decreasing temperature. They also found that the bed length did not affect D_e provided that the ratio of bed diameter to particle diameter was larger than 10. In a first attempt to study the mixing properties of single-phase flow in structured packings, Mak et al. (1991) presented axial dispersion coefficients in a pulsed packed column with water flowing through Sulzer SMV-12 structured packing. They found that D_e increased as the interstitial liquid velocity was increased, an expected result previously observed by other investigators using random packing.

Experimental Apparatus

Axial dispersion in packed beds can be measured independent of any mass transfer by the use of tracer injection techniques. This approach involves the injection into the inlet stream of an inert tracer by a step change, a sine wave, or a pulse. The evolution of the tracer concentration as a function of time is then monitored at some point downstream. The experimental approach used in the present investigation was based on the pulse injection method. The response of the tracer was measured at two different positions along the packed column. According to Aris (1959), this two-point measuring technique circumvents the need of a perfect tracer input, thus allowing a simplified experimental setup for the injection system. Another advantage of this scheme is that by locating the detection points far enough from the inlet and outlet of the packed section, end effects can be eliminated, or at least neglected.

Setup

The experimental apparatus consists of four main parts: the column and its accessories, the gas-and liquid-flow systems, the tracer injection system, and the tracer analysis system. The column and the flow control system form part of a pilot-scale unit originally designed for air stripping studies.

Axial dispersion studies were conducted in a circular column of 0.43 m ID and 6.69 m long (Figure 1). The column is constructed of glass fiber reinforced polyester, except for a

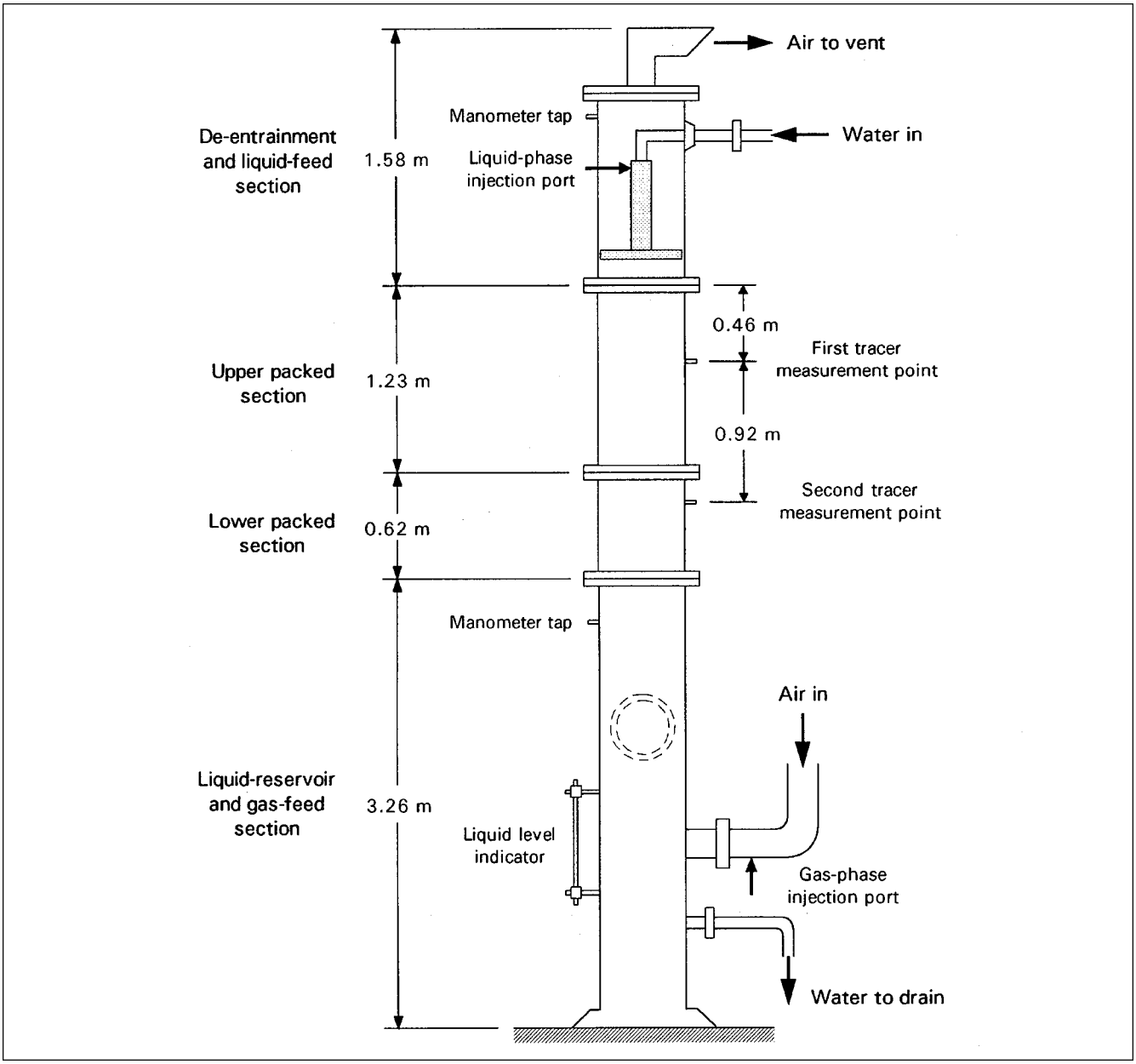

Figure 1. Test column.

clear Plexiglas section at the top to enable visual observation of the quality of liquid distribution to the bed. Air and water were the two contacting phases. The column was operated at atmospheric pressure and ambient temperature. Liquid was distributed through a perforated pipe device which provided 62 openings of 3.97 mm diameter, giving a pour point density of 430/m^2. The exit water discharged directly to a sanitary sewer. Ambient air was introduced below the bed through a multibeam injection support plate and was discharged at the top to the atmosphere. Two general types of packings were considered in the present study: random and structured.

Two random packings were selected according to their resistance to gas and liquid flow: 25.4-mm ceramic Raschig rings, a bluff-body type packing, and 25.4-mm metal Pall rings, a through-flow packing. Two representative structured packings were studied: Sulzer BX, fabricated from wire gauze, and Flexipac 2, made from sheet metal which has been fluted and perforated. The geometric properties of the four packings are given in Table 1. For more details on these packings, Kister (1992) may be consulted.

A flow diagram of the experimental system is shown in Figure 2. Signal outputs produced by the measuring devices were connected to a computerized control system which allowed a process variable of interest to be pre-set, maintained to a constant value, and continuously monitored. Air-flow rate was measured by an annubar and a differential-pressure cell transmitter. The inlet water (from the city main) was measured by an orifice plate. All temperatures were measured by thermocouple probes.

Table 1. Geometric Characteristics of Packings Used in this Work

	Random Packings	
	25.4-mm Raschig Rings	25.4-mm Pall Rings
Nominal size (mm)	25.4	25.4
Void fraction	0.74	0.94
Approx. surface area (m^2/m^3)	190	205
$d_p a_p$	4.83	5.21
Wall thickness (mm)	3.2	24 gage
Outside dia. and length (mm)	25.4	25.4
Approx. no. elements per m^3	47,700	49,600
Approx. weight per m^3 (kg)	670	480
Material	Ceramic	Stainless steel
	Structured Packings	
	Sulzer BX	Flexipac 2
Void fraction	0.90	0.93
Specific surface area (m^2/m^3)	492	223
Crimp height (mm)	6.35	12.45
Crimp base length (mm)	12.7	25.9
Crimp side length (mm)	8.89	18.03
Crimp angle (deg)	60	45
Equivalent diameter (mm)	7.18	14.1
$d_{eq} a_p$	3.53	3.14
Perforation size (mm)	3.97	3.97
Element height (mm)	171.45	298.45
Surface finish	gauze	fluted
Material	Stainless steel	Stainless steel

Sources: Vendor information and direct measurement.

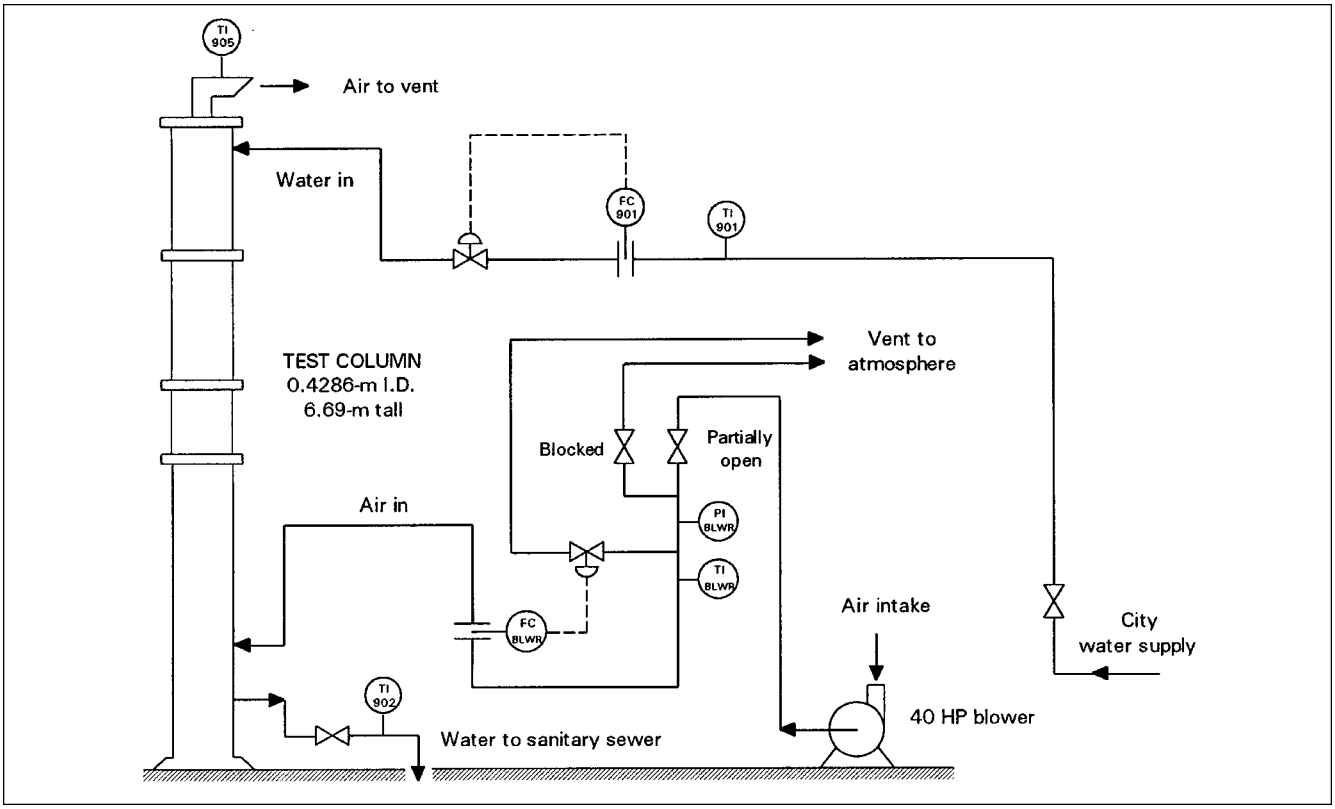

Figure 2. Gas- and liquid-flow system.

An injection system was devised for each phase to introduce pulses of tracer of arbitrary shape into the inlet streams. The gas-phase system is shown in Figure 3. Pulses of helium were injected into the inlet air upstream of the distributor, thus minimizing radial concentration gradients. To inject a pulse of helium into the inlet air, helium was allowed to flow to the injection cylinder by momentarily opening the on-off valve. The pressure in the injection cylinder was set to a predetermined value and the on-off valve was closed. The contents of the cylinder were then injected by energizing the solenoid-operated valve for a short period of time.

The liquid tracer injection system is shown in Figure 4. The tracer was an aqueous solution of 20%-wt. sodium chloride. The solution was circulated to ensure a uniform concentration, with a prescribed portion flowing through a rotameter to a three-way solenoid valve. When the solenoid was energized to switch for a short period of time, a pulse of tracer was injected into the liquid distributor. The duration of switch could be conveniently pre-set by a timing device. Figure 4 also shows the orientation of the injection line inside the liquid distributor; this arrangement minimized the effect of water flow on the tracer entry.

The tracer concentration in either phase was measured continuously at two different points downstream from the injection point. Each measuring point was axially positioned along the packed section of the column. The salt concentration was measured by electrical conductance, whereas the helium concentration was monitored by means of thermal conductivity. An especially-designed probe for each phase was used to measure the dynamic response of the tracer inside the packed bed. The distance between the top and the bottom probe was 0.92 m (see Figure 1). Small cylindrical cavities in the structured packing were created by an electrodischarge technique which disintegrated the metal; drilling the cavities would have deformed the packing elements to alter the flow distribution. For the random packings, special wire enclosures were used. All tracer measurements were made at the center of the cross section.

Two gas samplers were constructed to provide steady flow of gas from inside the bed to the thermal conductivity detectors (TCD). The tracer detection system in the gas phase is depicted in Figure 5. The voltage signals produced by the TCDs were processed and recorded through a data acquisition system.

The liquid tracer concentration was monitored *in situ*, using two custom-designed flow-through conductance cells. Each cell consisted of two platinum electrodes embedded in a cylindrical body made of Teflon which was inserted into a Plexiglas tube. This electrode arrangement with a cell constant of 0.3232 cm^{-1} was similar to that employed by Dunn et al. (1977). A sample volume of 5.6 mL was small enough to neglect the effect of mixing and dead time in the cell, giving an instantaneous detection of the flowing tracer solution. The response voltages of the conductance meters were connected directly to the recording system. Macías-Salinas (1995) gives more detailed information of the different samplers and detection systems used.

The output signals generated by the detectors and the timing device were recorded simultaneously by graphical and electronic means using a strip-chart recorder and a computer-based data acquisition system, respectively. The analog signals were fed into a digital data logger which comprised an I/O connector block, an analog/digital converter (ADC) board, and an IBM AT microcomputer. The data acquisition board consisted of a 12-bit successive-approximation ADC with eight analog inputs. The ADC board was configured in such a manner to handle three analog input channels: two for the tracer response curves and one for the injection mark.

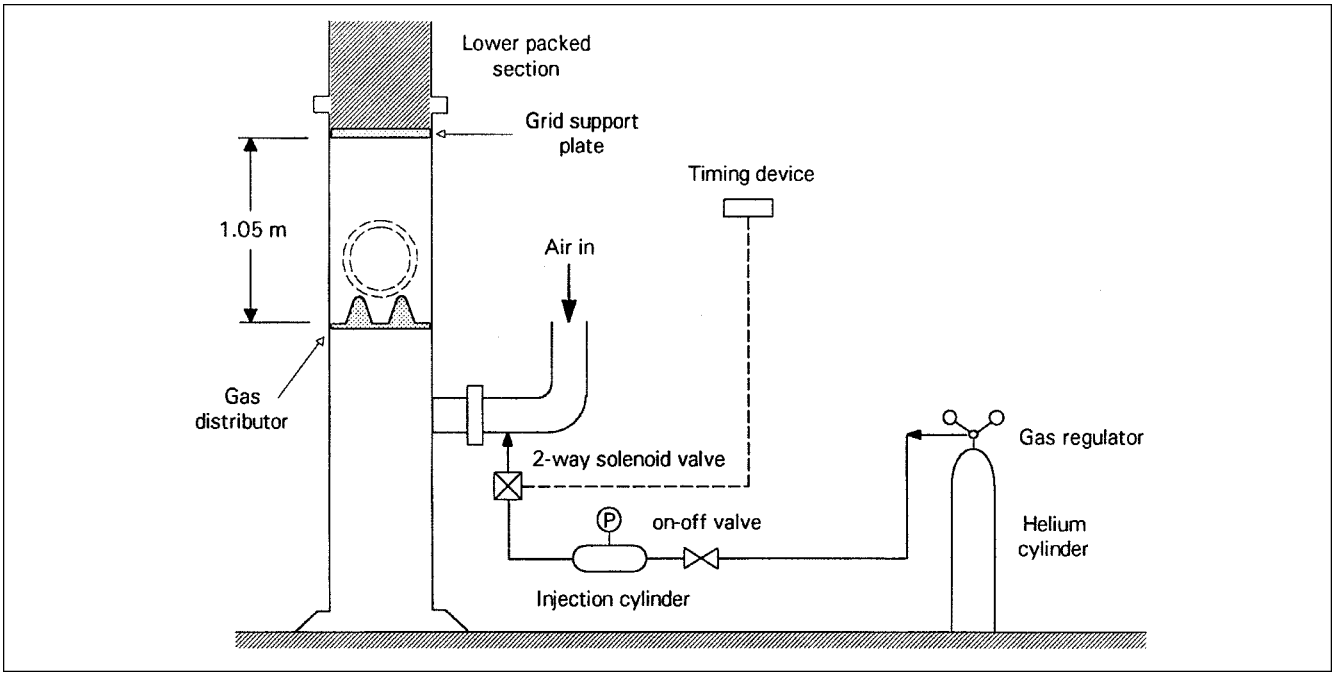

Figure 3. Gas-phase tracer injection system.

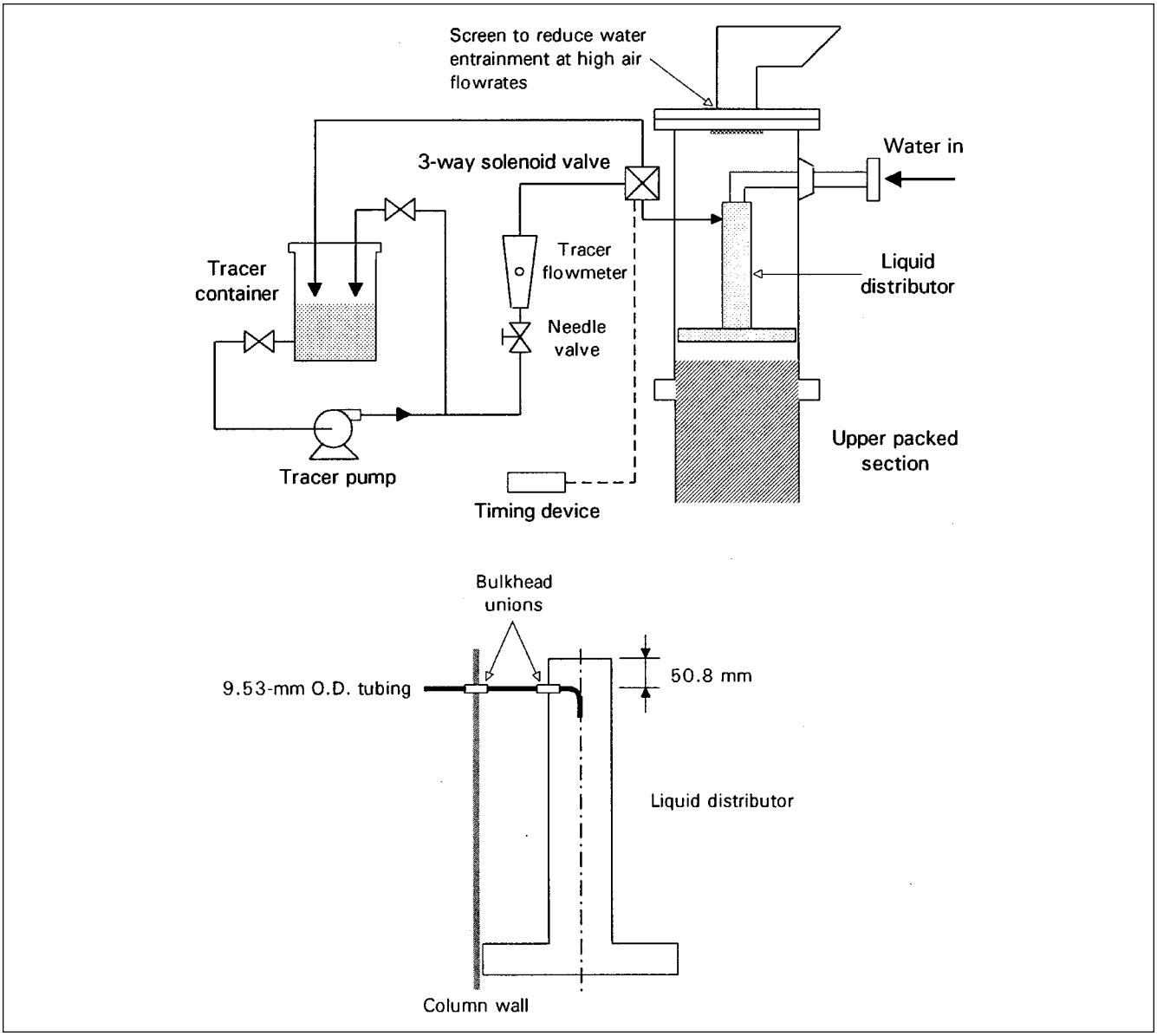

Figure 4. Liquid-phase tracer injection system.

The use of the ADC board allowed the collection of many data points per unit time (about 100 points/s), thus enhancing substantially the accuracy of the parameter estimation results (areas under the curve, first and second moments, and so on), particularly over the tails of the response curves.

Experimental procedure

Four parameters were varied in order to observe their effect on axial dispersion: gas-flow rate, liquid-flow rate, packing geometry, and time of tracer injection. The tracer experiments were conducted at liquid-flow rates of 3.25, 5, 6.75 and 8.5 kg/m^2·s. Gas-flow rates were varied from 0.4 to 4 kg/m^2·s. For a particular set of gas- and liquid-flow rates, the duration of tracer injection was varied within the ranges of 0.1 to 1 s and 1 to 2 s for the gas and liquid experiments, respectively. Prior to using the conductance cells, the electrodes of the cell were coated with platinum black to avoid polarization effects resulting from the relatively high conductivity of the tracer solution. See Macías-Salinas (1995) for more details on the experimental procedure.

Theoretical Model

Probably one of the most successful flow models is the diffusion-type model. Originally proposed by Danckwerts (1953), this model assumes that the complete dispersion phenomena can be decribed by replacing the molecular diffusion coefficient by an effective dispersion coefficient. The latter accounts for the combined mixing effects caused by molecular and turbulent eddy diffusion, as well as by transfer of material in and out of the stagnant zones created by portions of

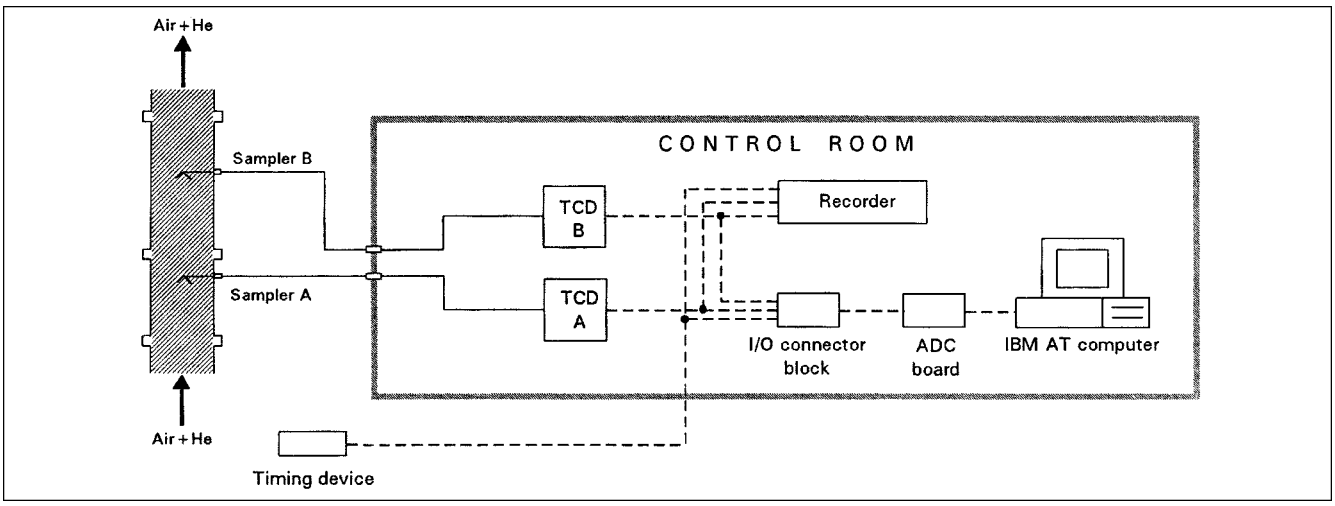

Figure 5. Gas-phase tracer detection system.

fluid trapped inside the packing interstices. The model is derived from a material balance for the tracer over an element $\pi r^2 dz$ of the packed bed. The resulting partial differential equation, based on a modified version of Fick's law, is

$$D_e \frac{\partial^2 C}{\partial z^2} - \nu \frac{\partial C}{\partial z} = \frac{\partial C}{\partial t} \tag{1}$$

where the axial dispersion coefficient D_e and the interstitial velocity ν are assumed to be independent of concentration C, position z (m) and time t (s) within the column. It is also assumed that no concentration gradients exist in the radial direction. As discussed by Kreft and Zuber (1978), the solution of the above equation depends greatly on the boundary conditions used. In general, the concentration is zero for any point inside the column before the tracer is injected. The second boundary condition has to do with the form of tracer input (step change, pulse or sine wave). The conditions at the outlet end of the column serve as the third boundary condition. For an infinite bed or open system, where the dispersion properties upstream of the tracer injection are the same as those within the packed column, the following initial and boundary conditions are used

$$C(z,0) = \frac{M}{A}\delta(z) \tag{2}$$

$$\lim_{z \to \pm\infty} C(z,t) = 0 \tag{3}$$

Based on the above conditions, Levenspiel and Smith (1957) presented an analytical solution of Eq. 1. At the exit of the test-section length (m) ($z = L$), the solution is

$$C = \frac{M}{A(4\pi D_e t)^{1/2}} \exp\left[-\frac{(L-\nu t)^2}{4D_e t}\right] \tag{4}$$

where M stands for the amount (kg) of tracer injected into the fluid and A is the cross-sectional area (m^2) of the column. In terms of dimensionless variables, Eq. 4 becomes

$$\frac{C}{(M/V)} = \left(\frac{Bo}{4\pi\theta}\right)^{1/2} \exp\left[-\frac{Bo(1-\theta)^2}{4\theta}\right] \tag{5}$$

where θ is the residence time and Bo is the dispersion or Bodenstein number, both defined as follows

$$\theta = \frac{\nu t}{L} \tag{6}$$

$$Bo = \frac{\nu L}{D_e} \tag{7}$$

The diffusion-type model can describe sufficiently the mixing behavior in packed columns ranging from perfect mixing ($Bo \to 0$) to plug flow ($Bo \to \infty$). The suitability of this model has been demonstrated by many investigators; however, as pointed out by Hennico et al. (1963), the model is incapable of giving an adequate description of axial dispersion in shallow beds. Other shortcomings include the inability to describe mixing phenomena resulting from fluid capacitance and nonflat velocity profiles.

In the present study, both gas- and liquid-phase residence time distribution (RTD) curves were interpreted in terms of the diffusion-type model (Eq. 1). This flow model was used because of its analogy to the diffusion equation and the possibility of utilizing all of the classical mathematical solutions that are available in the literature (Kreft and Zuber, 1978). Our experimental approach was based on the two-point measuring technique in which an imperfect pulse was injected and the response patterns were measured at two positions in the bed. This experimental arrangement suggests the use of an infinite packed bed as a boundary condition (see Figure 6).

If the initial tracer concentration is zero along the bed, the transfer function for an infinite packed bed, within a distance

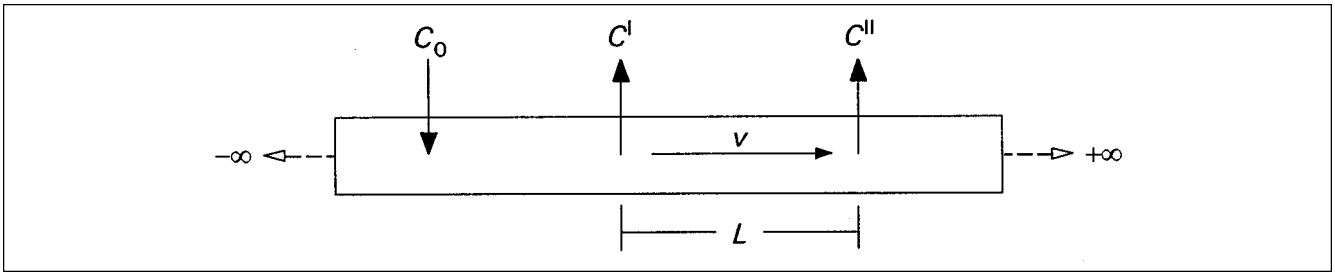

Figure 6. Experimental scheme for dynamic response studies in both phases.

L, can be related to the measured signals $C^{I}_{exp}(t)$ and $C^{II}_{exp}(t)$ by

$$F(s) = \frac{\int_0^\infty C^{II}_{exp}(t)\exp(-st)\,dt}{\int_0^\infty C^{I}_{exp}(t)\exp(-st)\,dt} \tag{8}$$

$$F(s) = \exp\left\{\frac{1}{2}Bo\left[1-\left(1+\frac{4\theta_m s}{Bo}\right)^{1/2}\right]\right\} \tag{9}$$

Equation 9 was derived by applying the Laplace transform to Eq. 4 representing the time-domain solution of the diffusion-type model for an open system. Various techniques have been used for the estimation of the packed bed parameters (θ_m and Bo) described by the diffusion model (Wakao and Kaguei, 1982; Macías-Salinas, 1995). Most of the estimation methods used in this work (method of moments, weighted moment method, Fourier analysis and transfer function fitting) deal with the measured tracer curves multiplied by a time function known as a weighting factor. Obviously, the best weighting factor is unity, that is the parameters are best determined by analysis in the time domain. In this method, the experimental RTD curves are compared to those predicted by the time domain solution of the diffusion-type model based on assumed parameter values. The prediction of the theoretical curve is made via a convolution integral

$$C^{II}_{cal}(t) = \int_0^t C^{I}_{exp}(\xi)\,f(t-\xi)\,d\xi \tag{10}$$

where $f(t)$ is the Laplace inversion of the transfer function. From Eq. 9, $f(t)$ is found to be

$$f(t) = \frac{1}{2\theta_m\left[\frac{\pi}{Bo}\left(\frac{t}{\theta_m}\right)^3\right]^{1/2}}\exp\left[-\frac{\left(1-\frac{t}{\theta_m}\right)^2}{\frac{4}{Bo}\frac{t}{\theta_m}}\right] \tag{11}$$

The best fit values of the model parameters θ_m and Bo are then obtained by minimizing the following objective function

$$G(\theta_m, Bo) = \left[\frac{\int_0^\infty\left(C^{II}_{exp}-C^{II}_{cal}\right)^2 dt}{\int_0^\infty\left(C^{II}_{exp}\right)^2 dt}\right]^{1/2} \tag{12}$$

where the righthand side of Eq. 12 represents the root-mean-square error between C^{II}_{exp} and C^{II}_{cal} over the entire range. A Fortran-77 program was written to calculate the mixing parameters θ_m and Bo via the parameter estimation methods described above. A complete description of the program is given by Macías-Salinas (1995).

Table 2. Reproducibility Errors of Observed RTD Curves in Gas Phase

		Parameter Estimation Method				
Packing	*R.M.S.E.*	MM	WMM	FA	TFF	TDF
25.4-mm Raschig Rings	min.	0.0132	0.0130	0.0092	0.0134	0.0092
	max.	0.0696	0.0670	0.0670	0.0693	0.0668
	avg.	0.0318	0.0296	0.0221	0.0311	0.0220
25.4-mm Pall rings	min.	0.0061	0.0059	0.0057	0.0061	0.0057
	max.	0.1137	0.0506	0.0599	0.0994	0.0529
	avg.	0.0547	0.0274	0.0209	0.0481	0.0202
Sulzer BX	min.	0.0283	0.0261	0.0139	0.0270	0.0139
	max.	0.0980	0.0469	0.0271	0.0942	0.0271
	avg.	0.0627	0.0343	0.0189	0.0559	0.0188
Flexipac 2	min.	0.0220	0.0170	0.0097	0.0199	0.0097
	max.	0.0880	0.0496	0.0337	0.0842	0.0323
	avg.	0.0436	0.0285	0.0172	0.0414	0.0171

MM = method of moments
WMM = weighted moment method
FA = analysis in the Fourier domain
TFF = transfer function fitting
TDF = curve fitting in the time domain

Results and Discussion

Gas phase: reproducibility of experimental RTD curves

All the experimental response curves in the gas phase exhibited slight asymmetry (tailing) indicating the existence of small amounts of dispersion. To obtain a quantitative measure of dispersion, the diffusion-type model (Eq. 1) was applied to the experimental data. The reproducibility results using the estimation methods mentioned above are listed in Table 2 for the four packings in terms of root-mean-square errors (RMSE) between the measured and theoretical RTD curves. According to these results, the model parameters determined via the Fourier and time domain analysis produced the smallest RMSE values for the four packings, while the

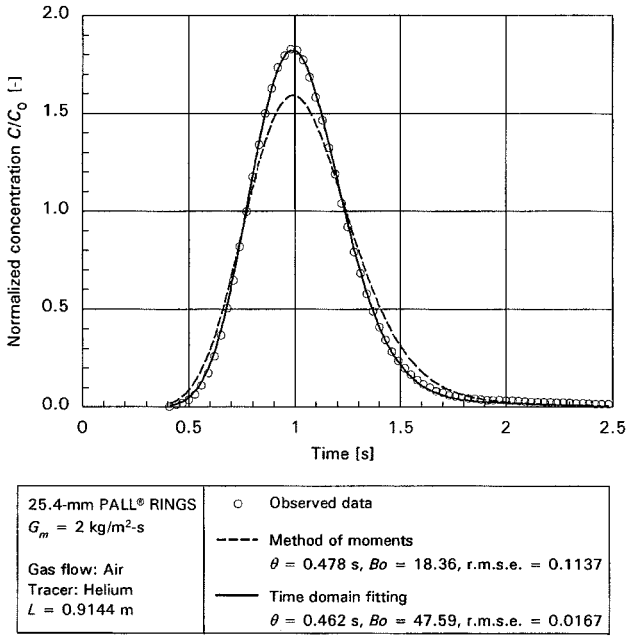

Figure 7. Reproducibility of the experimental RTD curve in the gas phase via two-parameter estimation methods.

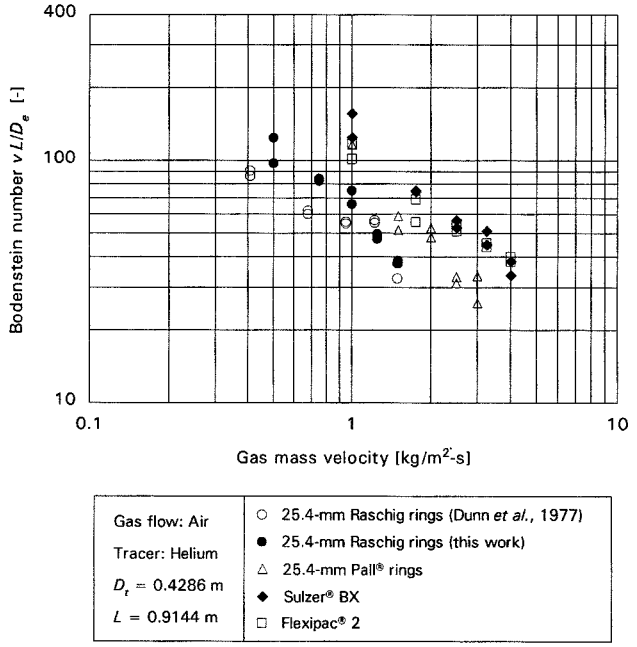

Figure 8. Gas-phase Bodenstein numbers vs. gas-flow rate.

method of moments yielded less accurate results with the highest reproducibility errors. Figure 7 depicts the inability of the method of moments as compared to the time domain fitting to reproduce the experimental response curve for metal Pall rings. This discrepancy is the result of small errors in the tailing portions of the curve. These errors are magnified in the evaluation of the second central moment used to estimate the dispersion number *Bo*. Accordingly, Bodenstein numbers *Bo* are in much wider disagreement than the mean residence times θ_m calculated by the two estimation methods.

Based on the general criterion that a good fitting is obtained at values of RMSE < 0.05, the agreement between the experimental RTD curves and those predicted using parameter values calculated by the five estimation methods is very close, as demonstrated by the average RMSE values listed in Table 2. The best model parameters were chosen as those that produced the smallest RMSE values. The success of the diffusion-type model in reproducing the response data so well can be explained by the resemblance of the experimental RTD curves to the classical Gaussian distribution, in the sense that the frontal and tailing portions of the curve are almost symmetrical.

Gas phase: axial mixing results

Figure 8 gives the experimental Bodenstein numbers for the four packings as a function of gas-flow rate. A measure of axial dispersion is represented by the value of the Bodenstein number *Bo*; as the value of *Bo* decreases, the amount of dispersion increases and vice versa. As shown, the degree of mixing in the gas phase was found to increase with the gas-flow rate for each packing. In general, dispersion of a gas flowing in a packed bed is considered to be the result of two main mechanisms: molecular diffusion and eddy (turbulent) diffusion. At low Reynolds numbers ($Re < 1$), dispersion is controlled by molecular diffusion, whereas at high Reynolds numbers ($Re > 10$), turbulent diffusion is the dominant factor affecting dispersion. The range of Reynolds numbers utilized in this work was extremely high (372 to 3,932). At these conditions, dispersion in the gas phase is entirely dominated by turbulence in the packing interstices.

The increase of mixing at high gas-flow rates can be therefore explained by the formation of more eddies in the flow channels. Levenspiel (1972) has given the following estimates for the degree of dispersion: small: $Bo \geq 500$, large: $Bo \leq 5$. According to these estimates, the range of Bodenstein numbers (26 to 156) obtained for all the packings indicates small-to-intermediate amounts of dispersion in the gas phase. As shown in Figure 8, the values of *Bo* for the two structured packings (Sulzer BX and Flexipac 2) are relatively higher than those obtained for the random packings at similar flow conditions. In packings of the structured type, the channels available for gas flow are regular in shape and more uniform in size than those of the random packings. This arrangement produces less dispersion due to a decrease of turbulence intensity. The random variation of the channel geometry in random packings can therefore explain the increased amount of dispersion in the gas phase for this type of packing. It can also be seen from Figure 8 that the dispersion levels exhibited by the Pall rings are smaller than those found in the Raschig rings. The superior aerodynamic properties and higher porosity of the Pall rings supports this finding. For comparison, the dispersion data of Dunn et al. (1977) for air flowing through 25.4-mm ceramic Raschig rings have also been plotted in Figure 8. The difference in magnitude be-

tween the two sets of data is attributed to the fact that Dunn and co-workers implicitly included end effects in their mixing results, thus resulting in low values of the Bodenstein number.

Gas phase: axial mixing correlations

Because of the lack of a fundamental theory for axial dispersion in packed beds, the results were correlated by means of equations derived from dimensional analysis. As depicted by Figure 7, the dispersion in the gas phase is mostly affected by the gas rate for each packing. The dispersion data of the two random packings can be correlated through the use of a single expression by including the effects of packing geometry. A geometry group widely used by many investigators is the product of the nominal diameter of the packing times the surface area of the packing $d_p a_p$ (values of this group can be found in Table 1). The form in which the dispersion data is influenced by this geometrical factor cannot be clearly determined (only two geometries were studied). A power-law dependence of Bo on $d_p a_p$ were therefore assumed

$$Bo = \alpha Re^{\beta} (d_p a_p)^{\gamma} \tag{13}$$

Since the porosity of the bed appears to influence the dispersion number, its effect was also incorporated into the above equation by expressing the Reynolds group in terms of the interstitial velocity of the gas ν

$$Bo = \alpha \left(\frac{\upsilon d_p \rho}{\eta} \right)^{\beta} (d_p a_p)^{\gamma} = \alpha Re_i^{\beta} (d_p a_p)^{\gamma} \tag{14}$$

where ν is evaluated from the mean residence time of the gas θ_m by

$$\nu = \frac{L}{\theta_m} \tag{15}$$

and L is the distance between the first and second measuring points. A multiple nonlinear regression analysis based on the Levenberg-Marquardt method served to fit the data of both packings to Eqs. 13 and 14. Table 3 gives the values of the regression constants and their 95% confidence limits. Both correlations gave the same predictive performance with similar standard deviations. It is important to note that the interstitial velocity in Eq. 14 had the same correlating effect as the superficial velocity, thus diminishing the importance of the bed porosity as a major independent variable. We conclude that the geometrical factor $d_p a_p$ can describe satisfactorily the experimental data in terms of differences in geometry between the two packings. The correlating form given by Eq. 13 is the easier to use, since it avoids the cumbersome calculation of the interstitial velocity from RTD experiments. The comparison of experimental Bo values with those predicted by this correlation is shown in a parity plot by Figure 9a. The correlation appears to be an adequate description of the experimental data showing low scatter.

The present correlated results for 25.4-mm ceramic Raschig rings have been compared with those of previous investigators. The majority of the investigators based their correlated results on the Péclet number or packing Bodenstein number

$$Pe = \frac{\nu d_p}{D_e} = Bo \frac{d_p}{L} \tag{16}$$

The above definition served to express Eq. 13 in terms of the Péclet number rather than the Bodenstein number. The correlation for 25.4-mm Raschig rings thus becomes

$$Pe = 819.23 Re^{-0.8551} \tag{17}$$

Figure 10 gives a graphical comparison of the gas-phase Péclet numbers predicted by Eq. 17 with those calculated from literature correlations for ceramic Raschig rings. Clearly there is disagreement among the results from the different correlations, particularly between those of DeMaria and White (1960) and Sater and Levenspiel (1966) for 12.7-mm Raschig rings. The use of different D_t/d_p ratios and experimental techniques may explain this discrepancy. Our correlation gives Péclet numbers that are about 26% to 53% larger than those obtained from the data of Dunn et al. (1977) for almost the same range of Reynolds numbers. This conflicts with the small differences observed between the results of both studies in terms of Bodenstein numbers which depend on the test section length. Dunn and co-workers used a test section 1.7 times longer than ours, thus giving lower values in the Péclet number (Eq. 16).

According to Figure 8, the two structured packings exhibited similar dispersion results. The general forms of Eqs. 13

Table 3. Results Obtained from Nonlinear Regression Calculations

	Parameters and 95% Confidence Limits					
Eq.	α	β	γ	φ	N	Std. Dev.
13	4.8198	-0.9958 ± 0.2	6.1503 ± 2.9	⋯	19	9.3274
14	689.704	-0.9698 ± 0.2	3.0589 ± 2.5	⋯	19	9.0839
19	4,036,890	-0.9177 ± 0.1	-3.8700 ± 1.3	⋯	20	8.2625
20	3,010,140	-0.9146 ± 0.1	-3.5741 ± 1.2	⋯	20	8.2597
34	705,383	0.9064 ± 0.3	-5.2732 ± 2.7	⋯	13	3.3396
35	4,621.56	0.7298 ± 0.5	-2.8545 ± 4.2	⋯	13	5.1970
37	352.341	1.9022 ± 0.9	5.7796 ± 3.1	8.4320 ± 11.0	14	3.5268
38	512.957	1.7417 ± 0.6	3.3003 ± 1.7	6.4591 ± 5.9	14	2.7522

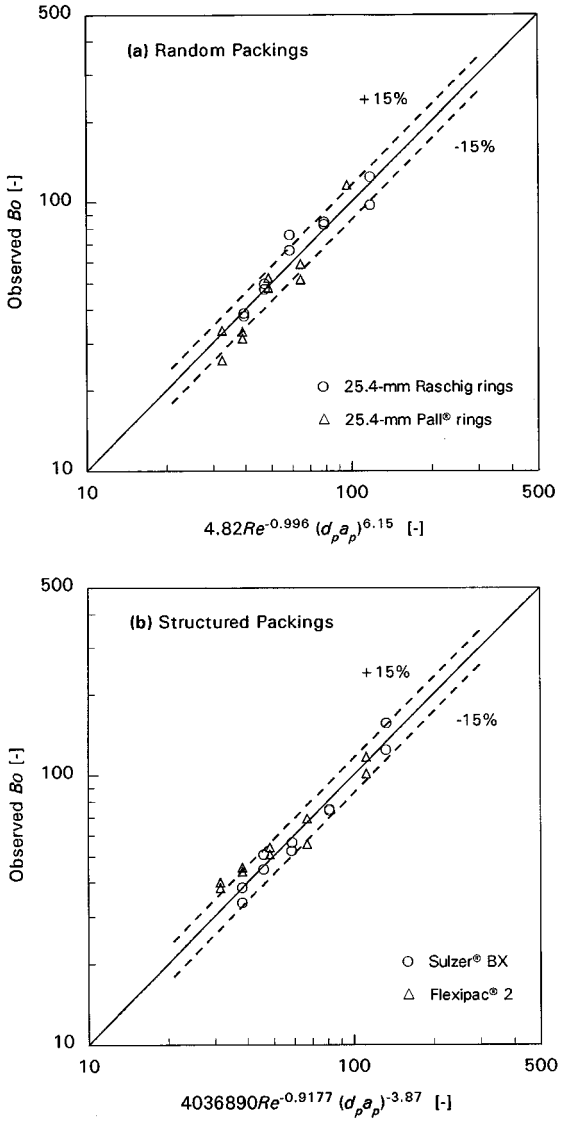

Figure 9. Experimental gas-phase Bodenstein numbers *Bo* vs. values calculated by correlations (a) random packings (Eq. 13); (b) structured packings (Eq. 19).

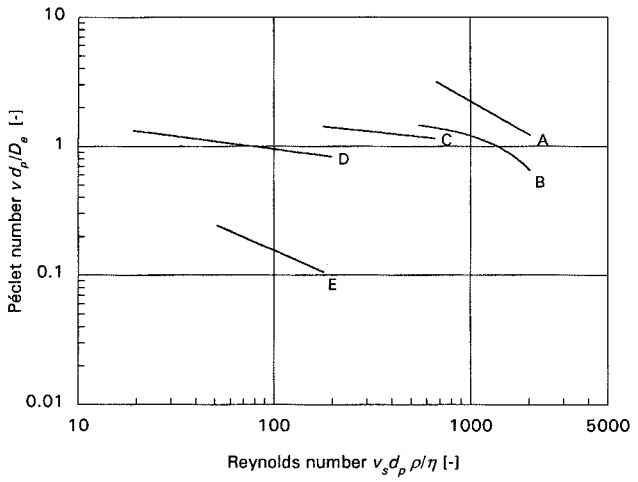

A: Present work $Pe = 819.23Re^{-0.8551}$	D: DeMaria and White (1960), 12.7-mm RR $Pe = 2.4Re^{-0.2}$
B: Dunn *et al.* (1977) $Pe = 1.7686 - 0.000559Re$	E: Sater and Levenspiel (1966), 12.7-mm RR $Pe = 3.4Re^{-0.67}$
C: Burghardt and Bartelmus (1979) $Pe = 10(d_p/d_t)^{0.6185}Re^{-0.163}$	

Figure 10. Results of this work vs. gas-phase Péclet numbers from correlations by other authors (12.7- and 25.4-mm Raschig rings).

and 14 were also used to correlate these results. The special geometry of the structured packing suggested, however, the use of a different characteristic length in the Reynolds group. The equivalent diameter (m) d_{eq} of the flow channels, which characterizes the size and shape of the structured packing, was used. Bravo et al. (1985) give the following definition of d_{eq} based on the corrugation dimensions of the structured packing

$$d_{\mathrm{eq}} = Bh\left[\frac{1}{B+2S} + \frac{1}{2S}\right] \qquad (18)$$

where B is the channel base (m), h is the crimp height (m), and S is the channel side (m). These dimensions are given in Table 1. Equation 18 represents the arithmetic average of two hydraulic radii derived from a triangle and a diamond. The following correlation forms were therefore used to regress the data into a single expression

$$Bo = \alpha\left(\frac{\nu_s d_{\mathrm{eq}}\,\rho}{\eta}\right)^{\beta}\left(d_{\mathrm{eq}}a_p\right)^{\gamma} = \alpha Re^{\beta}\left(d_{\mathrm{eq}}a_p\right)^{\gamma} \qquad (19)$$

$$Bo = \alpha\left(\frac{\nu d_{\mathrm{eq}}\,\rho}{\eta}\right)^{\beta}\left(d_{\mathrm{eq}}a_p\right)^{\gamma} = \alpha Re_i^{\beta}\left(d_{\mathrm{eq}}a_p\right)^{\gamma} \qquad (20)$$

where the interstitial velocity ν (m/s) must be evaluated from the mean residence time of the gas obtained from the RTD curve. The correlating constants along with the 95% confidence limits derived from a nonlinear regression analysis of the data are given in Table 3. The results show that both correlations have the same predictive capabilities. The correlating form of Eq. 19 is preferred since it eliminates the need of calculating the interstitial velocity from RTD curves. Figure 9b gives the comparison between the experimental dispersion data and those predicted by Eq. 19. As shown, the difference between the observed and predicted values varies within the 15% range with low scatter. Note that although the values of d_{eq} and a_p change appreciably between the two packings, there is only a very slight variation of the value of $d_{\mathrm{eq}}a_p$ (see Table 1). In consequence, the degree of dependence of the Bodenstein number on the packing geometry is weak for this particular case. This explains the similarity in dispersion results obtained for both packings (Figure 8).

Table 4. Reproducibility Errors of Observed RTD Curves in Liquid Phase

Packing	R.M.S.E.	Parameter Estimation Method				
		MM	WMM	FA	TFF	TDF
25.4-mm Raschig rings	min.	0.0361	0.0330	0.0309	0.0345	0.0309
	max.	0.1344	0.1349	0.1088	0.1968	0.1065
	avg.	0.0821	0.0555	0.0535	0.0653	0.0497
25.4-mm Pall rings	min.	0.0700	0.0447	0.0359	0.0466	0.0358
	max.	0.1734	0.0963	0.0918	0.1306	0.0891
	avg.	0.1103	0.0661	0.0591	0.0776	0.0571
Sulzer BX	min.	0.0264	0.0267	0.0226	0.0349	0.0225
	max.	0.1042	0.0922	0.0914	0.1712	0.0760
	avg.	0.0718	0.0558	0.0496	0.0917	0.0459
Flexipac 2	min.	0.0400	0.0322	0.0291	0.0365	0.0260
	max.	0.0976	0.0812	0.0745	0.1123	0.0743
	avg.	0.0601	0.0504	0.0483	0.0680	0.0447

MM = method of moments
WMM = weighted moment method
FA = analysis in the Fourier domain
TFF = transfer function fitting
TDF = curve fitting in the time domain

Liquid phase: reproducibility of experimental RTD curves

Unlike the RTD curves in the gas phase, the response curves obtained in the liquid phase exhibited long tailing portions. This strong tailing tendency, often found in packed-bed RTD curves, is mainly caused by elementary mechanisms, such as split of the liquid rivulets by the packing and, retention and remixing of some tracer elements within the packing voids. For the experimental conditions used in this work (trickle flow without gas flow), the RTD curves in the liquid phase also showed large contents of random noise, particularly at the lowest liquid rate. This scatter resulted from the irregularities of the liquid films entering the sampling section of the conductance cell. The scatter in the tailing portion of the curves played an important role on the degree of reproducibility of the experimental data via the diffusion-type model.

For the four packings, Table 4 lists the reproducibility results in terms of root-mean-square errors (RMSE) between the experimental and predicted response curves, using the parameter estimation methods outlined above. The performance of three of the four estimation methods that use weighting factors (method of moments, weighted moment method, and transfer function fitting) was adversely affected by the experimental errors in the tailing portion of the curves, thus producing the highest RMSE values for all the packings. The exception was the Fourier analysis that along with the time domain analysis yielded the best reproducibility results. Figure 11 illustrates the superior characteristics of the time domain analysis over the method of moments in reproducing the measured response curves. From Table 4, the reproducibility errors for the two structured packings were relatively smaller than those obtained for the random packings. The regular geometry of the structured packing may explain this finding: a more uniform liquid flow can be attained. Despite the strong asymmetry of the response curves, the use of the diffusion-type model produced acceptable reproducibility results with an average RMSE value of 0.0494 for all the packings.

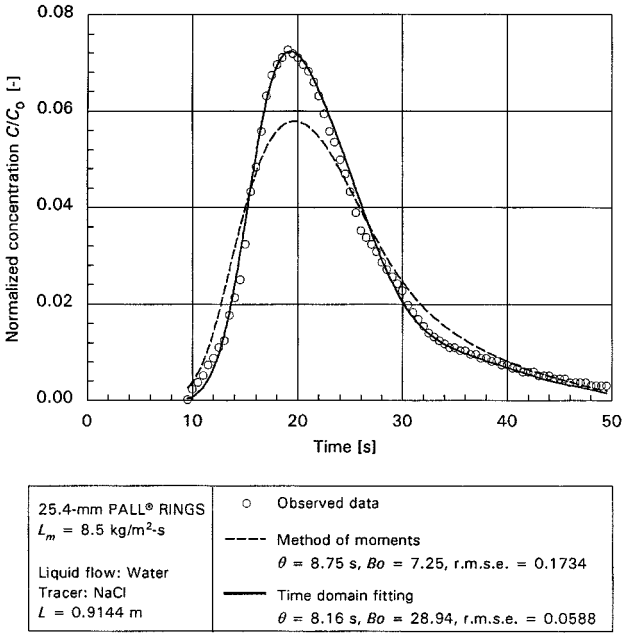

Figure 11. Reproducibility of the experimental RTD curve in the liquid phase via two parameter estimation.

Liquid-phase results

Liquid Holdup. The volume fraction of the bed occupied by the liquid expressed in terms of total liquid holdup H_t can be evaluated from the mean residence time θ_m

$$H_t = \frac{\nu_s \theta_m}{L} \tag{21}$$

where ν_s is the superficial velocity (m/s) of the liquid and L is the test section length. The total holdup is the sum of the static holdup (m^3/m^3) H_s and the dynamic holdup (m^3/m^3) H_d. The static holdup represents the portion of liquid that remains stagnant within the packing interstices due to capillary forces. It is thought to be independent of the liquid flow rate and to change only with the packing characteristics. The static holdup is in part responsible for the long tailing portions found in the experimental RTD curves. However, not all the response curves exhibited similar tails in length. The tailing tendency was more pronounced at low liquid rates suggesting an increased liquid stagnation. Since the static holdup remains constant at any liquid loading, the only way to explain the above finding is that the mass exchange between the stagnant liquid and the mobile phase (dynamic holdup) is slower, thus causing longer tails at low liquid rates. Values of total holdup are shown in Figure 12 for the four packings. It can be seen that total holdup increases as the liquid rate is increased, with similar tendencies for all the packings. Of the four packings, Sulzer BX produced by far the highest mean residence times due to the capillary nature of the gauze material that allows an excellent wetting of the large surface area of the packing. The consistency of the liquid holdup data was checked by comparing our values for the

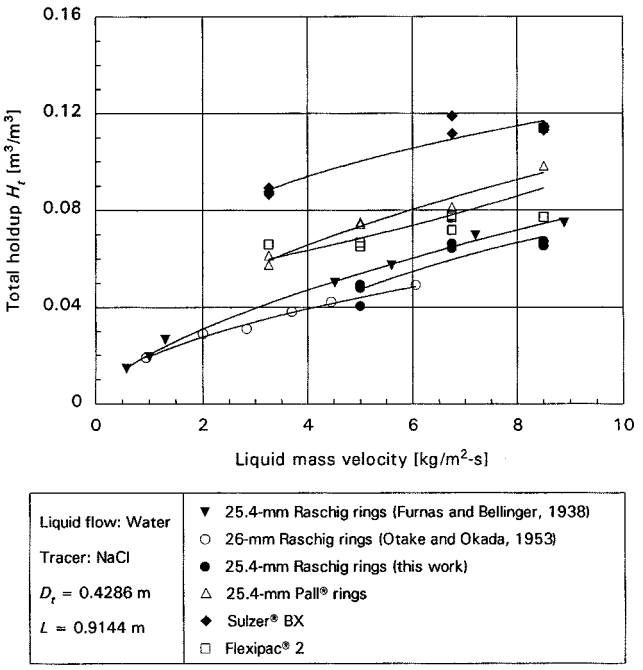

Figure 12. Total liquid holdup vs. liquid rate.

25.4-mm ceramic Raschig rings with those reported by previous investigators using the volumetric approach. It is evident that the present holdup data for ceramic Raschig rings is in good agreement with those published earlier.

Axial Mixing. The axial mixing results in the liquid phase for each packing are presented in Figure 13 in terms of Bodenstein numbers at different liquid rates. In contrast to the gas-phase results, axial mixing in the liquid phase decreases with increasing the liquid rate. The reproducibility of the dispersion data is only fair. Part of the scatter may be ascribed to the difficulty of locating the truncation point in the tailing portion of the RTD curves. The range of measured Bodenstein numbers (7 to 40) indicates the existence of intermediate-to-large dispersion levels in the liquid phase according to the estimates for the degree of dispersion given above. For the experimental conditions used in this work, we may conclude that the liquid phase exhibits more departure from plug-flow conditions than does the gas phase. This is an expected finding, since the liquid flow behavior appears to be most affected by hydraulic factors such as wall effects, nonuniform distribution of the liquid, and bed capacitance (liquid retention in static holdup).

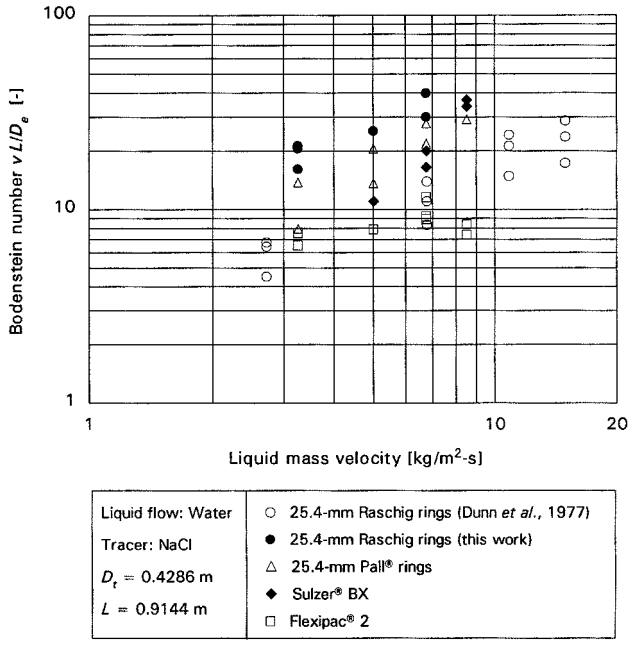

Figure 13. Liquid-phase Bodenstein numbers vs. liquid-flow rate.

Surprisingly, the 25.4-mm ceramic Raschig rings produced the lowest mixing results with the highest Bodenstein numbers. Two possible explanations: first, the good wetting characteristics of the ceramic material promotes a better spread of the liquid in the packing. For this situation, the RTD curves should become more symmetrical, resulting in increased values of the Bodenstein number. Second, the high interstitial velocity of the liquid in packings of low porosity reduces the local mixing due to the small residence times of the fluid elements. On the other hand, the largest levels of axial dispersion in the liquid phase were exhibited by Flexipac 2, another unexpected result. Also, it can be seen from Figure 13 that the dependence of the Bodenstein number on the liquid-flow rate was much less pronounced for Flexipac 2 than for the other packings. Some possible causes may be: (1) poor wetting of the packing area within the present range of liquid rates, leading to irregular flow paths and insufficient spread of the liquid in the channels; (2) the existence of a large number of mixing crossings between the flow channels; and (3) the effect of the inclination angle of the flow channels in the sense that a small inclination angle with the horizontal decreases the component of gravitational force that pulls the liquid film downward, resulting in a lower film velocity. The inclination angles for Sulzer BX and Flexipac 2 are 60° and 45° with the horizontal, respectively. Thus, the inclination angle may play an important role in the dispersion behavior of both packings. The mixing data of Dunn et al. (1977) for water flow through 25.4-mm ceramic Raschig rings are also plotted in Figure 13 for comparison purposes. Clearly, there is a significant disagreement. The larger degrees of axial dispersion found by Dunn et al. may possibly be attributed to their experimental measurements that implicitly included end effects.

Liquid-phase correlations

(a) Total Holdup. Liquid holdup under trickle flow conditions without gas flow is mostly affected by liquid flow variables (flow rate and physical properties), local gravitational acceleration, and shape of the packing. A dimensional analysis was successfully applied by Otake and Okada (1953) to express their dynamic holdup results in terms of the above variables. The general form of their correlation is given by

$$H_d = \alpha\left(\frac{\nu_s d_p \rho}{\eta}\right)^{\beta}\left(\frac{d_p^3 \rho^2 g}{\eta^2}\right)^{\gamma}\left(d_p a_p\right)^{\varphi}$$

$$= \alpha Re^{\beta} Ga^{\gamma}\left(d_p a_p\right)^{\varphi} \quad (22)$$

where the Galileo group Ga ($d_p^3 \rho^2 g/\eta^2$) includes the effect of the acceleration due to gravity g (m/s^2). We used a similar form in reproducing our total holdup results for random packings, as a function of the two major independent variables: liquid flow rate and packing geometry. The value of Ga remained fairly constant, however, as a result of the liquid density and viscosity not changing. There were small differences in gravitational forces acting on the liquid films (both packings consisted of rings of equal size). This suggested the use of the combined group $H_t Ga^{1/3}$ to correlate the results

$$H_t Ga^{1/3} = \alpha Re^{\beta} \left(d_p a_p \right)^{\gamma} \tag{23}$$

A multivariable regression analysis yielded the following relationship

$$H_t = 0.000817 Re^{0.5442} Ga^{-1/3} \left(d_p a_p \right)^{4.945} \tag{24}$$

where the 95% confidence limits of the regression exponents β and γ are ± 0.15 and ± 1.23, respectively. As shown by Figure 14a, the above equation satisfactorily correlates the experimental data for both packings with a standard deviation of 0.0043 based on 13 data points. However, it is evident that Eq. 24 cannot be used to predict static holdup by extrapolating H_t at zero liquid flow rate. It is only valid within the range of liquid flow rates considered in this study (3.25–8.5 kg/m^2·s).

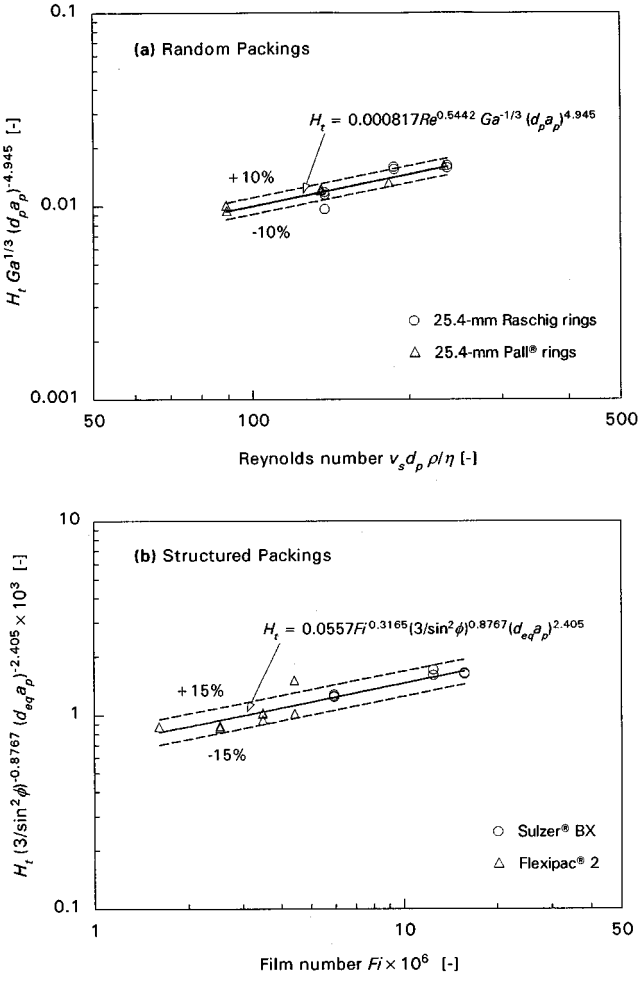

Figure 14. Total liquid holdup of this work vs. those from correlations (a) random packings (Eq. 24); (b) structured packings (Eq. 32).

A somewhat different form of the holdup correlation proposed by Otaka and Okade (1953) was used to express the results of both structured packings as a function of liquid flow rate, inclination angle of the flow channels and packing geometry. The new correlation also contains dimensionless groups and was derived from the following definition for dynamic holdup

$$H_d = a_p \Delta \tag{25}$$

where a_p is the surface area (m^2/m^3) of the packing partially covered by liquid films of thickness (m) Δ flowing down the column. Assuming the liquid films to be uniform in size and flow at constant velocity over a flat surface inclined to the horizontal with an angle (deg) ϕ, Shi and Mersmann (1985) presented a Nusselt-type expression for Δ based on laminar flow of the film

$$\Delta = \left(\frac{3\eta L_m^*}{\rho^2 g \sin\phi} \right)^{1/3} \tag{26}$$

where the term $g \sin\phi$ represents the effective gravity acting on the liquid film in the channel direction (Rocha et al., 1993) and L_m^* is the liquid mass-flow rate in kg/m·s width of surface

$$L_m^* = \frac{L_m}{a_p \sin\phi} = \frac{\nu_s \rho}{a_p \sin\phi} \tag{27}$$

Combining Eqs. 25–27, the expression for H_d becomes

$$H_d = \left(\frac{3\eta a_p^2 \nu_s}{\rho g \sin^2\phi} \right)^{1/3} \tag{28}$$

The righthand side of the above equation may be written in terms of three dimensionless groups as follows:

$$H_d = \left(\frac{\eta \nu_s}{d_{eq}^2 \rho g} \right)^{1/3} \left(\frac{3}{\sin^2\phi} \right)^{1/3} \left(d_{eq} a_p \right)^{2/3} \tag{29}$$

The size and shape of the channels are accounted for by the combined effect of the last two groups. The first is referred to as the film number ($\eta\nu_s/d_{eq}^2 \rho g$) Fi and is equal to the ratio of the Froude number ($\nu_s^2/g d_{eq}$) Fr to the Reynolds number Re

$$Fi = \frac{Fr}{Re} = \frac{\nu_s^2/g d_{eq}}{\nu_s d_{eq} \rho/\eta} \tag{30}$$

According to the above equation, at low Reynolds numbers (low velocity or high viscosity losses), viscous forces predomi-

nate as the resistance to gravity on the liquid films. In general, the gravity-viscosity and gravity-inertia regimes occurs at high and low values of the film number, respectively. Equation 29 served as the basis for correlating the total holdup results for the two structured packings. The correlating form is given by

$$H_t = \alpha Fi^{\beta}\left(\frac{3}{\sin^2\phi}\right)^{\gamma}\left(d_{\mathrm{eq}}a_p\right)^{\varphi} \tag{31}$$

The correlation obtained from a multiple regression analysis of the data is

$$H_t = 0.0557Fi^{0.3165}\left(\frac{3}{\sin^2\phi}\right)^{0.8767}\left(d_{\mathrm{eq}}a_p\right)^{2.405} \tag{32}$$

where the 95% confidence limits of the exponents were 0.3165 ± 0.15, 0.8767 ± 0.55, and 2.405 ± 1.97. As shown by Figure 14b, the experimental results are described acceptably by Eq. 32 with a standard deviation of 0.0088 based on 16 data points. To verify the consistency of the present correlation with Eq. 29, a multiple regression analysis was performed on the data with the proportionality factor α equal to unity. This yielded the following results

$$H_t = Fi^{0.3165}\left(\frac{3}{\sin^2\phi}\right)^{0.3871}\left(d_{\mathrm{eq}}a_p\right)^{0.6541} \tag{33}$$

The values of the exponents in Eqs. 33 and 29 are similar, thus confirming the suitability of Eq. 29 for describing liquid holdup in packings of the structured type.

(b) Axial Dispersion Number. In view of the lack of a fundamental theory for axial dispersion in packed beds, the present mixing results were correlated using equations obtained from dimensional analysis of the pertinent operating variables. Since both liquid holdup and axial mixing depend on the liquid flow pattern and packing geometry, the same correlating forms for liquid holdup can therefore be used to describe the dispersion results obtained in this work. For random packings, a correlating form similar to Eq. 23 was used to express the Bodenstein numbers as a function of the liquid flow rate and packing geometry

$$BoGa^{1/3} = \alpha Re^{\beta}\left(d_p a_p\right)^{\gamma} \tag{34}$$

As mentioned earlier, the Galileo number Ga was not a correlating variable; it remained almost unchanged for the two packings. The effects of liquid holdup can be incorporated implicitly into the above equation by expressing the Reynolds group in terms of the interstitial velocity of the liquid ν

$$BoGa^{1/3} = \alpha\left(\frac{\nu d_p \rho}{\eta}\right)^{\beta}\left(d_p a_p\right)^{\gamma} = \alpha Re_i^{\beta}\left(d_p a_p\right)^{\gamma} \tag{35}$$

where ν can be either evaluated from RTD experiments or calculated using the holdup correlations given here (noting that $\nu = \nu_s H_t^{-1}$). Table 3 gives the results from a multiple nonlinear regression of the data using Eqs. 34 and 35. The results show that there was not an apparent improvement in using the interstitial velocity of the liquid as a correlating variable. The additional scatter introduced by the experimental ν values may explain the high standard deviation in Eq. 35. The comparison of experimentally determined dispersion numbers with values calculated from the best correlation (Eq. 34) is shown in Figure 15a. The agreement appears to be acceptable and within $\pm 15\%$ of difference in most cases.

A large number of correlations for ceramic Raschig rings have been reported in the literature dealing with axial dispersion in the liquid phase. The dispersion results provided by the majority of these correlations are given in terms of the Péclet number. To compare the present correlated results for Raschig rings with those of previous investigators, Eq. 34 was

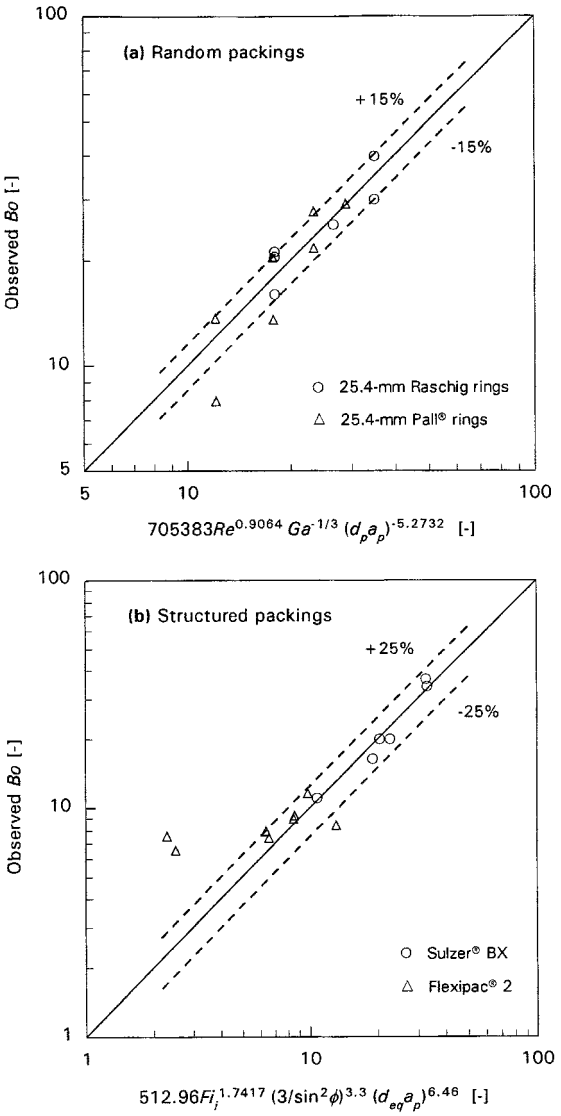

Figure 15. Experimental liquid-phase Bodenstein numbers *Bo* vs. values calculated by correlations (a) random packings (Eq. 34); (b) structured packings (Eq. 38).

expressed in terms of the Péclet number (Eq. 16)

$$Pe = 0.0128\,Re^{0.8551} \tag{36}$$

Figure 16 shows the comparison between the results predicted by the above equation and those correlated by other investigators for Raschig rings of similar size. As shown, there is a significant discrepancy in the dispersion results estimated by the various correlations. This disagreement may be attributed to the combined effects of factors such as preferential flow of the liquid to the column walls due to low values of column/packing diameter ratio and, use of different experimental techniques and methods of data analysis. For example, the correlations of Co and Bibaud (1971) and von Stockar and Cevey (1984) are in wide disagreement despite the fact that both investigators utilized similar D_t/d_p ratios, large enough to neglect wall effects. However, unlike Co and Bibaud, von Stockar and Cevey safely neglected end effects in their tracer measurements by employing the two-point detection technique. In general, failure to eliminate end effects properly may lead to overestimation of the amount of mixing with low values of the Péclet number. Consistent with this explanation is the correlation of Dunn et al. (1977) which implicitly includes end effects.

In the case of structured packings, it appears that the major independent variables affecting dispersion are the superficial velocity of the liquid v_s, the inclination angle ϕ of the channels, and size of the flow channels d_{eq}. The correlating form of Eq. 31 was used to express our dispersion results

$$Bo = \alpha Fi^{\beta}\left(\frac{3}{\sin^2\phi}\right)^{\gamma}\left(d_{eq}a_p\right)^{\varphi} \tag{37}$$

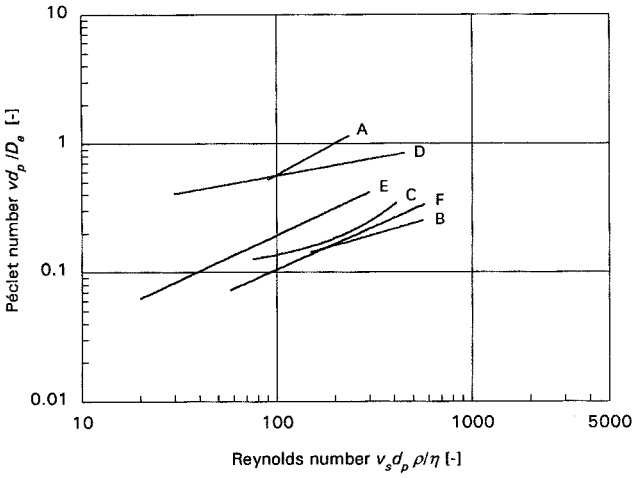

A: Present work $Pe = 0.0128Re^{0.8551}$	D: von Stockar and Cevey (1984) $Pe = 1.32Re^{0.27}\,Ga^{-0.11}$
B: Co and Bibaud (1971) $Pe = 0.0165Re^{0.4313}$	E: Sater and Levenspiel (1966), 12.7-mm RR $Pe = 0.00758Re^{0.703}$
C: Dunn *et al.* (1977) $Pe = 0.1011 \cdot 10^{0.001304Re}$	F: Choe and Lee (1985), 12.7-mm RR $Pe = 3.342Re^{0.669}\,Ga^{-0.344}$

Figure 16. Results of this work vs. liquid-phase Péclet numbers computed from correlations of other authors (12.7- and 25.4-mm Raschig rings).

where the effects of the liquid velocity are included in the Film number *Fi* according to Eq. 30. Another important correlating variable is the interstitial velocity of the liquid ν which incorporates the effects of liquid holdup. One can also express Eq. 37 in terms of this variable

$$Bo = \alpha\left(\frac{\eta\nu}{d_{eq}^2\rho g}\right)^{\beta}\left(\frac{3}{\sin^2\phi}\right)^{\gamma}\left(d_{eq}a_p\right)^{\varphi} \tag{38}$$

where

$$\nu = \frac{L}{\theta_m} = \frac{\nu_s}{H_t} \tag{39}$$

The results from a multiple regression analysis based on Eqs. 37 and 38 are given in Table 3. The results suggest that there is little dependence of the dispersion number on the geometrical factor $d_{eq}a_p$, as evidenced by the high confidence limits of its exponent φ. Although the values of d_{eq} and a_p vary widely between the two packings, the corresponding values of the geometrical factor are similar. It can be therefore deduced that the group $d_{eq}a_p$ accounts only for the shape of the packing, that is, for packings of similar shape: $d_{eq}a_p \approx k$, a dimensionless constant. This explains the slight effect of $d_{eq}a_p$ on the Bodenstein number resulting from the triangular shape of the flow channels in both packings. This also establishes the importance of the inclination angle of the channels as a correlating variable. On the other hand, Eq. 38 turned out to be the best correlation with the lowest standard deviation. The use of the interstitial velocity in Eq. 38 can be therefore justified because of the large difference in holdup values between Sulzer BX and Flexipac 2. Figure 15b shows the ability of Eq. 38 to correlate the dispersion data of the two structured packings. The scatter of the data indicates that the present correlation appears to describe satisfactorily most of the data points, particularly those of Sulzer BX.

Conclusions

Axial mixing characteristics of a single-phase flow were determined experimentally for a second-generation random packing and two structured packings using a large-scale column. Liquid holdup data were also obtained. The following conclusions can be drawn from this work:

- The results confirmed previous mixing observations made by other investigators using first-generation random packings: the liquid exhibits more departure from plug flow than the gas within the present range of flow conditions; axial mixing in the gas increased with gas-flow rate whereas liquid-phase axial mixing was a decreasing function of liquid rate.
- The two-parameter mixing model provided to be a suitable means of describing axial mixing in both phases owing to the excellent reproducibility of the response curves. Despite the strong tailing portions exhibited in the liquid phase, the performance of the model in this case was also good.
- Liquid holdup values obtained in this work via tracer tests are in good agreement with previous measurements based on the volumetric method.

Table 5. Qualitative Rank-Order Comparison of Dispersion Level for Four Packings Studied

Level of Axial Dispersion	*Single-Phase Flow*	
	Gas Phase	*Liquid Phase*
Highest (low *Bo*)	RR1	FLEX2
	PR1	SULBX
	FLEX2	PR1
Lowest (high *Bo*)	SULBX	RR1

RR1 = 25.4-mm Raschig rings, PR1 = 25.4-mm Pall rings, SULBX = Sulzer BX, FLEX2 = Flexipac 2.

- A qualitative rank-order comparison of the dispersion level for the four packings studied is summarized in Table 5.
- The lowest mixing effects in the gas were obtained for the two structured packings owing to their higher bed porosity and uniform variation of their channel geometry.
- Surprisingly, Flexipac 2 structured packing produced the highest levels of axial mixing in the liquid. It is thought that poor wetting of the packing area at the present range of liquid rates along with the 45° inclination angle of the flow channel may produce an adverse mixing effect in this packing.
- A power-law dependence between the dispersion numbers *Bo* in both phases and the major operating variables was found to describe adequately the experimental results. The agreement between the results from the correlations presented here and experimental data was good, with most of the points varying within the $\pm 20\%$ difference range with moderate scatter.
- A new correlating form was developed to reproduce holdup and mixing data of the two structured packings. This correlation incorporates the inclination angle of the channel as a major independent variable (Eqs. 31 and 37), thus reflecting the distinctive mixing mechanisms occurring in random and structured packings.
- Because of the complexity of flow behavior in packed beds, the axial dispersion numbers determined in this work should be regarded only as an approximation of the quantitative effect of local axial and radial dispersion, as well as wall flow.
- To minimize axial mixing effects, better packing designs should be considered. For example, a high-porosity packing with regular flow channels may reduce axial dispersion in the gas. For the liquid, packings having good wettability properties may promote low levels of axial mixing. For structured packings, based on the present results, an inclination angle of the flow channels less than 60° should be avoided.

Acknowledgment

The authors wish to thank the Separations Research Program at The University of Texas at Austin, and the National Council of Science and Technology of México (CONACyT) for providing financial support for this research.

Notation

α, β, γ = regression constants
δ = Dirac delta function
η = viscosity, kg/m·s
φ = regression constant
ρ = density, kg/m^3
ξ = dummy time variable, s
C_0 = normalized tracer concentration at time zero
d_p = nominal diameter (random packing), m
D_t = column diameter, m
$F(s)$ = transfer function in the Laplace domain
G = objective function in the dime domain
G_m = gas-flow rate, kg/m^2·s
h = crimp height, m
H_t = total liquid holdup, m^3/m^3
L^* = characteristic length, m
L_m = liquid flow rate, kg/m^2·s
r = radial distance coordinate, m
s = Laplace operator, s^{-1}
V = volume of column, m^3

Subscripts

cal = predicted value
exp = measured value
p = packing

Superscripts

I = first measuring point
II = second measuring point

Literature Cited

Arts, R., "Notes on the Diffusion-Type Model for Longitudinal Mixing in Flow," *Chem. Eng. Sci.*, **9**, 266 (1959).
Bravo, J. L., J. A. Rocha, and J. R. Fair, "Mass Transfer in Gauze Packing," *Hydrocarb. Proc.*, **64**, 91 (1985).
Burghardt, A., and G. Bartelmus, "Experimental Determination of Longitudinal Dispersion in Two-Phase Flow through Packing," *Chem. Eng. Sci.*, **34**, 405 (1979).
Cairns, E. J., and J. M. Prausnitz, "Longitudinal Mixing in Packed Beds," *Chem. Eng. Sci.*, **12**, 20 (1960).
Carberry, J. J., and R. H. Bretton, "Axial Dispersion of Mass in Flow Through Fixed Beds," *AIChE J.*, **4**, 367 (1958).
Choe, D. K., and W. K. Lee, "Liquid Phase Dispersion in a Packed Column with Countercurrent Two-Phase Flow," *Chem. Eng. Commun.*, **34**, 295 (1985).
Co, P., and R. Bibaud, "Longitudinal Mixing of the Liquid Phase in Packed Columns with Countercurrent Two Phase Flow," *Can. J. Chem. Eng.*, **49**, 727 (1971).
Danckwerts, P. V., "Continuous Flow Systems. Distribution of Residence Times," *Chem. Eng. Sci.*, **2**, 1 (1953).
DeMaria, F., and R. R. White, "Transient Response Study of Gas Flowing Through Irrigated Packing," *AIChE J.*, **6**, 473 (1960).
Dunn, W. E., T. Vermeulen, C. R. Wilke, and T. T. Word, "Longitudinal Mixing in Packed Gas-Absorption Columns," *Ind. Eng. Chem. Fundam.*, **16**, 116 (1977).
Ebach, E. A., and R. R. White, "Mixing of Fluids Flowing Through Beds of Packed Solids," *AIChE J.*, **4**, 161 (1958).
Edwards, M. F., and J. F. Richardson, "Gas Dispersion in Packed Beds," *Chem. Eng. Sci.*, **23**, 109 (1968).
Evans, E. V., and C. N. Kenney, "Gaseous Dispersion in Packed Beds at Low Reynolds Numbers," *Trans. Instn. Chem. Engrs.*, **44**, T189 (1966).
Furnas, C. C., and F. Bellinger, "Operating Characteristics of Packed Columns," *Trans. AIChE J.*, **34**, 251 (1938).
Hennico, A. N., G. L. Jacques, and T. Vermeulen, "Longitudinal Dispersion in Packed Extraction Columns," *U.S. Atomic Energy Comm.*, Rept. UCRL-10696 (1963).
Kister, H. Z., *Distillation Design*, McGraw-Hill, New York (1992).
Kramers, H., and G. Alberda, "Frequency Response Analysis of Continuous Flow Systems," *Chem. Eng. Sci.*, **2**, 173 (1953).
Kreft, A., and A. Zuber, "On the Physical Meaning of the Dispersion Equation and Its Solutions for Different Initial and Boundary Conditions," *Chem. Eng. Sci.*, **33**, 1471 (1978).
Kunugita, E., T. Otake, and K. Yoshii, "Holdup and Mixing Coefficients of Liquid Flowing through Irrigated Packed Beds," *Chem. Eng. (Japan)*, **26**, 672 (1962).

Levenspiel, O., *Chemical Reaction Engineering*, 2nd ed., Wiley, New York (1972).
Levenspiel, O., and W. K. Smith, ''Notes on the Diffusion-Type Model for the Longitudinal Mixing of Fluids in Flow,'' *Chem. Eng. Sci.*, **6**, 227 (1957).
Liles, A. W., and C. J. Geankoplis, ''Axial Diffusion of Liquids in Packed Beds and End Effects,'' *AIChE J.*, **6**, 591 (1960).
Macías-Salinas, R., ''Gas- and Liquid-Phase Axial Dispersion through Random and Structured Packing,'' PhD Diss., The University of Texas at Austin (1995).
Mak, A. N. S., C. A. J. Koning, P. J. Hamersma, and J. M. H. Fortuin, ''Axial Dispersion in Single-Phase Flow in a Pulsed Packed Column Containing Structured Packing,'' *Chem. Eng. Sci.*, **46**, 819 (1991).
McHenry, K. W., and R. H. Wilhelm, ''Axial Mixing of Binary Gas Mixtures Flowing in a Random Bed of Spheres,'' *AIChE J.*, **3**, 83 (1957).
Miller, S. F., and C. J. King, ''Axial Dispersion in Liquid Flow Through Packed Beds,'' *AIChE J.*, **12**, 767 (1966).
Otake, T., and K. Okada, ''Liquid Holdup in Packed Towers (Operating Holdup without Gas Flow),'' *Chem. Eng.* (*Japan*), **17**, 176 (1953).
Rocha, J. A., J. L. Bravo, and J. R. Fair, ''Distillation Columns Containing Structured Packings: A Comprehensive Model for Their Performance: 1. Hydraulic Models,'' *Ind. Eng. Chem. Res.*, **32**, 641 (1993).
Sater, V. E., and O. Levenspiel, ''Two-Phase Flow in Packed Beds. Evaluation of Axial Dispersion and Holdup by Moment Analysis,'' *Ind. Eng. Chem. Fundam.*, **5**, 86 (1966).
Shi, M. G., and A. Mersmann, ''Effective Interfacial Area in Packed Columns,'' *Ger. Chem. Eng.*, **8**, 87 (1985).
Strang, D. A., and C. J. Geankoplis, ''Longitudinal Diffusivity of Liquids in Packed Beds,'' *Ind. Eng. Chem.*, **50**, 1305 (1958).
Tan, C. S., and D. C. Liou, ''Axial Dispersion of Supercritical Carbon Dioxide in Packed Beds,'' *Ind. Eng. Chem. Res.*, **28**, 1246 (1989).
Urban, J. C., and A. Gomezplata, ''Axial Dispersion Coefficients in Packed Beds at Low Reynolds Numbers,'' *Can. J. Chem. Eng.*, **47**, 353 (1969).
Von Stockar, U., and P. F. Cevey, ''Influence of the Physical Properties of the Liquid on Axial Dispersion in Packed Columns,'' *Ind. Eng. Chem. Process Des. Dev.*, **23**, 717 (1984).
Wakao, N., and S. Kaguei, *Heat and Mass Transfer in Packed Beds*, Gordon and Breach Science Publishers, New York (1982).

Manuscript received Apr. 16, 1998, and revision received Nov. 17, 1998.